Mon. Not. R. Astron. Soc. **000**, 1–12 (XXXX) Printed 30 September 2014 (MN LATEX style file v2.2)

Hydrogen delivery onto white dwarfs from remnant exo-Oort cloud comets

Dimitri Veras[1⋆], Andrew Shannon[2], Boris T. Gänsicke[1]
[1] *Department of Physics, University of Warwick, Coventry CV4 7AL, UK*
[2] *Institute of Astronomy, University of Cambridge, Cambridge CB3 0HA, UK*

arXiv:1409.7691v1 [astro-ph.SR] 26 Sep 2014

Accepted 2014 September 26. Received 2014 September 26; in original form 2014 June 19

ABSTRACT

The origin of trace hydrogen in white dwarfs (WDs) with He-dominated atmospheres is a long-standing problem, one that cannot satisfactorily be explained by the historically-favoured hypothesis of accretion from the interstellar medium. Here we explore the possibility that the gradual accretion of exo-Oort cloud comets, which are a rich source of H, contributes to the apparent increase of trace H with WD cooling age. We determine how often remnant exo-Oort clouds, freshly excited from post-main-sequence stellar mass loss, dynamically inject comets inside the WD's Roche radius. We improve upon previous studies by considering a representative range of single WD masses ($0.52 - 1.00 M_{\odot}$) and incorporating different cloud architectures, giant branch stellar mass loss, stellar flybys, Galactic tides and a realistic escape ellipsoid in self-consistent numerical simulations that integrate beyond 8 Gyr ages of WD cooling. We find that $\sim 10^{-5}$ of the material in an exo-Oort cloud is typically amassed onto the WD, and that the H deposits accumulate even as the cloud dissipates. This accumulation may account for the relatively large amount of trace H, $10^{22} - 10^{25}$ g, that is determined frequently among WDs with cooling ages $\geqslant 1$ Gyr. Our results also reaffirm the notion that exo-Oort cloud comets are not the primary agents of the metal budgets observed in polluted WD atmospheres.

Key words: stars: white dwarfs – Oort Cloud – comets: general – stars: AGB and post-AGB – stars: evolution – The Galaxy: kinematics and dynamics

1 INTRODUCTION

The high surface gravity of white dwarfs (WDs) implies that their atmospheres are chemically stratified by atomic weight, and the lightest element floating on top will determine their spectroscopic appearance (Schatzman 1958). About 80% of the entire WD population have H-dominated (DA) atmospheres (Koester 2013). The remaining fraction of WDs have lost their residual H, most likely in a late shell flash (Althaus et al. 2005), and have He-dominated (DB) atmospheres.

Exquisite compositional analyses from the last few decades have emphasized that reality often departs from that simple picture: between a quarter to one half of all WD atmospheres show traces of metals (Zuckerman et al. 2003, 2010; Koester et al. 2014), and up to half of all He-atmosphere WDs contain varying amounts of trace-H (Dufour et al. 2007; Voss et al. 2007; Bergeron et al. 2011)[1]. Two important questions then are (1) from where do the metals originate? (2) what causes the apparent changes in the mass of H as a function of age? The historic answer to both questions is accretion from the interstellar medium (ISM, e.g. Wesemael 1979; Alcock & Illarionov 1980), but this hypothesis has major shortcomings that we discuss below.

Regarding the first question, the diffusion time scale of these elements in WD atmospheres is short compared to their cooling ages (Fontaine & Michaud 1979; Paquette et al. 1986; Koester 2009; see also Fig. 1 of Wyatt et al. 2014). Therefore, the spectroscopic detection of elements heavier than H and He does indeed unambiguously require ongoing or recent accretion. However, the theory that the accretion originated from the ISM encountered a substantial number of problems: (1) the small magnitude of the expected accretion rate from the ISM, (2) the sparse distribution of massive in-

⋆ E-mail:d.veras@warwick.ac.uk

[1] The spectra of WDs with mixed atmospheres are classified according to the strength of the observed lines, e.g. DBA for He-dominated atmospheres with a small amount of hydrogen. The presence of metals is indicated by adding the letter "Z", e.g. DAZ for a metal-polluted H-dominated star, or DZ for a featureless cool He-atmosphere with detectable metal lines (Sion et al. 1983).

© XXXX RAS

terstellar clouds, and (3) the existence of metal-rich but H-poor DBZ and DZ WDs (Aannestad et al. 1993; Friedrich et al. 2004; Jura 2006; Kilic & Redfield 2007; Farihi et al. 2010). Instead, the presence of metals has been explained by the tidal breakup and accretion of rocky material (Graham et al. 1990; Jura 2003; Bear & Soker 2013; Veras et al. 2014a) which subsequently form discs that accrete directly onto the WD (Jura 2008; Rafikov 2011a,b; Metzger et al. 2012; Rafikov & Garmilla 2012; Wyatt et al. 2014). Further supporting this thesis are actual detections of dozens of dust discs (Zuckerman & Becklin 1987; Becklin et al. 2005; Kilic et al. 2005; Reach et al. 2005; Farihi et al. 2009; Bergfors et al. 2014), several gaseous discs (Gänsicke et al. 2006, 2007, 2008; Gänsicke 2011; Farihi et al. 2012; Melis et al. 2012) and discs containing both dust and gas (Brinkworth et al. 2009; Melis et al. 2010; Brinkworth et al. 2012; Wilson et al. 2014).

The second question has received less attention, and is the primary motivation for this study. Hydrogen, being the lightest element, never sinks, but it can be subject to convective mixing (Koester 1976; Vauclair et al. 1979). Taken at face value, the mass of trace H detected in a substantial fraction of He-dominated WDs, derived from the analysis of optical spectroscopy and detailed envelope models, is found to monotonically increase from $M_{\rm H} \simeq 10^{14}$ g at a cooling age of a few 100 Myr to $M_{\rm H} \simeq 10^{25}$ g at 2 Gyr[2] (Dufour et al. 2007; Voss et al. 2007; Jura et al. 2009; Bergeron et al. 2011; see Fig. 7 of Raddi et al. 2014). While this distribution of $M_{\rm H}$ is biased by both physical effects (the depth of the He convection zone) and observational limitations, there is strong evidence that the oldest WDs carry the largest amount of trace-H (Dufour et al. 2007). Bergeron et al. (2011) demonstrate that this age-dependent distribution of trace-H, in particular the existence of relatively old WDs with extremely low values of $M_{\rm H}$, is incompatible with both primordial H left over from post-main sequence evolution and interstellar accretion. Stone et al. (2014) suggest that trace H in old WD atmospheres can be used to constrain exo-Oort clouds and the manner in which they are dynamically perturbed.

In this paper, we explore the long-term contribution to the H budget by the accretion of comets from exo-Oort clouds. We outline the general context of our arguments in Section 2. In Section 3, we discuss the interplay of forces relevant to our setup, and why we utilise numerical simulations in this work. Section 4 provides a detailed description of those simulations, and Section 5 illustrates the results. We conclude with a discussion in Section 6 and a summary in Section 7.

2 COMETS AS EXTERNAL ACCRETORS

2.1 Lessons from WD pollution

Much of the recent observational and theoretical work on WD pollution in evolved planetary systems has focused on the accretion of metals, for the simple reason that the detection of photospheric metals is a smoking gun of recent or ongoing accretion, in many cases accompanied by the simultaneous detection of the circumstellar reservoir of dusty and gaseous debris.

The nature of the parent bodies can be inferred from a compositional analysis of the debris, where the abundance of C is of particular importance: the mass fraction of C is $\simeq 24\%$ for comet Halley, whereas it is $\simeq 3.5\%$ for CI chondrites, 0.24% for the Sun, and $\simeq 0.1\%$ for the bulk Earth (Jessberger et al. 1988, Allègre et al. 2001, Lodders 2003, Asplund et al. 2009, see also Figure 14 of Klein et al. 2010).

Detailed abundance studies have been carried out so far only for a relatively small number of WDs (Zuckerman et al. 2007; Klein et al. 2010, 2011; Gänsicke et al. 2012; Jura et al. 2012; Xu et al. 2013, 2014). However, in all cases, the debris was found to be strongly depleted in C with respect to CI chondrites and hence incompatible with accretion by material with a composition similar to Solar system comets, regardless of the origin of these comets.

An independent method was pursued by Jura & Xu (2010, 2012) who interpreted the amount of trace-H in a sample of He-dominated WDs within 80 pc of the Earth originating from the accretion of planetary debris, and concluded that the parent bodies were typically dry, with a water content of at most $\sim 1-10\%$. Exceptions do exist (Farihi et al. 2013; Raddi et al. 2014) but represent distinct outliers (Fig. 7 of Raddi et al. 2014), and can be explained by asteroids which retain water throughout the main sequence and giant branch phases of the parent star's lifetime (Jura & Xu 2010).

In conclusion, the observational evidence in the above studies strongly favours the accretion of rocky, asteroid-like debris over exo-Oort cloud comets. However, *one bias that all these studies have in common is that they only addressed relatively young WDs*, with cooling ages $\lesssim 300$ Myr. The accretion of these comets may be less frequent and more challenging in terms of direct detection when compared to asteroids, but could still have a noticeable and observable long-term effect on the properties of WDs.

2.2 Lessons from the Solar system

Observed collisions of small bodies with the Sun, which is an almost 5 Gyr-old main sequence star, may help us understand the collision frequency with small bodies at ~ 5 Gyr-old WD cooling ages. What we see locally, however, does not necessarily agree with our current understanding of metal-polluted WD systems.

Comets impact the Sun frequently. In fact, coronographs like those part of SoHO's LASCO reveal that a comet grazes the Sun every few days, with a total of about 2400 grazers from 1996 to 2008 (Lamy et al. 2013). However, about 90% of these comets are from a single family (Kreutz) and have similar pericentres (about two Solar radii) and other orbital parameters. Further, the number of comets counted is a strong function of their brightness (Sekanina & Kracht 2013), and the observations do not provide physical parameters such as mass and radius. Nevertheless, large pieces of the Kreutz comet have been observed from the ground for centuries, and the estimated mass of the progenitor is at least 0.5×10^{20} g (Table 1 of Knight et al. 2010). By comparing this value to the heavy element mass in DBZ WDs that was accreted over the last 1 Myr or so years (Fig. 9 of Girven et al. 2012), we see that the Kreutz comet by itself

[2] The Balmer lines become increasingly weaker with increasing cooling age / decreasing temperature, as most H in the atmosphere is in the ground state. Consequently, it is extremely difficult to determine the amount of trace H in He-dominated WDs older than ~ 2 Gyr.

could explain the lowest accreted masses within just the last few hundred years. This result is independent of the comet's fragmentation frequency, number and type (sublimation-, ablation- or explosion-dominated; see Brown et al. 2011).

Contrastingly, asteroids infrequently graze the Sun. The grazing or collisional timescale is on the order of Gyr (Minton & Malhotra 2010); even asteroids in unstable resonances have collisional timescales of $\sim$ Myr (Table 1 of Gladman et al. 1997).

2.3 Our new contribution

This disagreement between observations inside and outside of our Solar System acts as a secondary motivation for our study, in addition to explaining the increasing mass of trace-H found among He-dominated WDs with time.

In a pioneering early investigation, Alcock et al. (1986) estimated that a exo-Oort cloud comet hits a WD about every 10^4 years, a value subsequently adopted by studies such as Debes & Sigurdsson (2002) and Zuckerman et al. (2007). In an extension of Alcock et al. (1986), Parriott & Alcock (1998) used the same underlying mass loss rate, but with an additive fictitious force to model asymmetric mass loss. They found that for an asymmetry which imparts an impulsive kick to the star on the scale of hundreds of m/s, the comet accretion rate is reduced. Stone et al. (2014) also adopts impulsive kicks, yielding accretion rates which span several orders of magnitude depending on the adopted kick velocities and pericentres (see their Fig. 1).

In this work, we extend the study of Alcock et al. (1986) by using a numerical integrator which includes flybys, tides, a realistic escape ellipsoid, stellar evolution profiles from a different dedicated stellar evolution code, a relevant range of progenitor stellar masses, and different radial profiles of exo-Oort cloud comets. Given the uncertainty in the mass of exo-Oort clouds and the limited resolution of numerical integrations, our primary output will be a fraction of comets which reach the Roche radius of the WD. From this value, one can determine a mass accretion rate by making assumptions about the mass of the comets and cloud.

3 RELEVANT FORCES

Throughout a star's lifetime, comets in an exo-Oort cloud are perturbed by both Galactic tides and stellar flybys. If a comet exits the star's gravitational sphere of influence, then the comet has escaped into the interstellar medium. Similarly, comets already in the interstellar medium may enter the star's gravitational sphere of influence. The sphere of influence is technically not a sphere, but rather a triaxial ellipsoid whose three axes are given analytically by equations (21-22) of Veras et al. (2014b).

We do not know the extent of the reservoir of interstellar comets. However, a few dedicated studies provide some estimates. Table 2 of Moro-Martín et al. (2009) indicates that the number density of comets outside of an exo-Oort cloud is about $10^7 - 10^9$ comets per cubic parsec. If the cloud itself contains about 10^{11} comets in an annulus extending from 10^4 au to 10^5 au, then the density within the cloud is 5×10^{10} comets per cubic parsec. Hence, the cloud itself is a few orders of magnitude more dense than its surroundings. Also, Jura (2011) importantly notes that no observed Sun-grazing comets have hyperbolic orbits, meaning that they all originated from inside of the Solar System. He places a specific constraint on interstellar comets with radii between 10 m and 2 km, claiming that they compose less than 1% of all interstellar oxygen. Further, interstellar comets have relative velocities on the order of 10 km/s, whereas Oort cloud comets instead have velocities which are at least one order of magnitude less. Hence, the star's gravity sets the path of its own comets, and bends interstellar comets towards it significantly only if they come within a few au. Overall, all these arguments help us justify neglecting capture of interstellar comets in this work.

When the star leaves the main sequence and evolves along giant branches, another important force affects the orbit of these comets: stellar mass loss. When the star becomes a WD, mass loss effectively ceases. The timescale for cometary orbits to change due to mass loss is much shorter than the timescale for changes due to the Galactic tide (Veras et al. 2014b). Consequently, these forces are effectively decoupled.

Given their large orbits ($10^4 - 10^5$ au in semimajor axis), all long-period comets will nonadiabatically respond to stellar mass loss (Veras et al. 2011). By *nonadiabatic* we mean that the behaviour is not simply described by a constant-eccentricity orbit expansion, as would be true for objects (such as planets) within a few hundred au of their parent stars. A comet's actual response to the mass loss is well described by a set of orbital element evolution equations in both the isotropic mass loss case (equations 35-37 of Omarov 1962 and equation 29 of Hadjidemetriou 1963) and anisotropic mass loss case (equations 18-23 and 34-38 of Veras et al. 2013b). Both cases demonstrate that cometary orbits will evolve in a non-obvious manner, featuring both decreases and increases in their eccentricities depending on their other orbital parameters.

The importance of anisotropy in mass loss was highlighted by Parriott & Alcock (1998) but not fully described with orbital elements in terms of the variable mass flux at different positions on the stellar surface until Veras et al. (2013b). The latter study highlights two important points: (1) if anisotropy exists, its importance scales as the square root of the semimajor axis, and (2) physically-sensible scaling laws for mass ejecta as functions of stellar latitude and co-longitude predict no net anisotropic effect whatsoever (their equations 51-53). These same laws, however, fail to reproduce observations which feature clearly asymmetrical structures like planetary nebulae (e.g. Kimeswenger et al. 2008). Hence, our knowledge of stellar physics still remains insufficient to adopt any particularly representative asymmetric mass loss prescription along the giant branches.

The general equations of motion for the two-body problem with mass loss and Galactic tides have no known analytic solution. Hence the correlation, for example, between initial conditions and escape from the Oort cloud is complex (see Figs. 10-11 of Veras & Wyatt 2012). However, useful dependencies can be extracted by analysing their form with orbital elements. For example, Veras et al. (2011) prove that the pericentre of a comet can never decrease while the parent star is losing mass isotropically. Heisler & Tremaine (1986), Brasser (2001) and Veras & Evans (2013) show that in the Solar neighbourhood, a comet whose orbit is coplanar with the Galactic disc

robustly resists changes to its semimajor axis and eccentricity because the Galactic vertical tide vanishes.

Nevertheless, these relationships may be significantly modulated in the presence of a flyby star. Kaib & Raymond (2014) particularly emphasise the importance of including stellar flybys for calculations of extremely close pericentre passages. The geometric details and impact parameters of flybys around stars other than the Sun is unknown. Even for the Sun, flyby trajectories can be computed only for a few Myr and only for a fraction of the stars in the Solar neighbourhood (Jiménez-Torres et al. 2011). Such uncertainty is compounded by the prospect of flyby binaries or flyby planetary systems (Veras & Moeckel 2012). A flyby can affect an orbiting planet in a variety of ways. Hence, in concert with Galactic tides, perturbations can force back down the pericentre of a comet which is raised by stellar mass loss.

4 NUMERICAL SIMULATIONS

This investigation determines the extent of the effects detailed in the last section, with important implications for WD pollution. The above discussion, coupled with the fact that energy is not conserved in mass-losing systems, suggests that a purely analytic approach is not feasible. Therefore, we turn to numerical simulations.

4.1 Integration procedure

In order to self-consistently model mass loss, Galactic tidal perturbations and multiple stellar flybys in an N-body integrator, we have heavily modified the integrator suite `Mercury` (Chambers 1999). The modifications include the following.

- We incorporate stellar mass loss into the code by splicing in-between Bulirsch-Stoer timesteps, which although is perhaps not necessary for test particle systems like ours here (Veras et al. 2011), significantly increases the accuracy for multiple massive objects (see Fig. 1 of Veras et al. 2013a).
- When the star is not losing mass, the standard non-conservative Bulirsch-Stoer integrator is still used because the perturbation on a comet due to a flyby may be arbitrarily large. When perturbations are large, symplectic integrators may become inaccurate.
- Stellar flybys are modelled as perturbative accelerations to all of the comets and the parent star. A new flyby is introduced when a probability threshold is reached after an individual timestep.
- We incorporate into the code the same prescription for Galactic tides as in Veras & Evans (2013) and Shannon et al. (2014a,b) and assume our modeled systems reside in the Solar neighbourhood, specifically at 8 kpc from the Galactic centre. We include both horizontal and vertical tides, and contributions from an exponential disc, a Hernquist bulge, and a cored isothermal halo.
- Because pollution likely arises from disrupted bodies forming discs or rings around the star, we replace the actual WD radius with the WD Roche radius. This change may significantly affect results relating to close encounters with the star (Mustill et al. 2014).
- We explicitly incorporate the Hill escape ellipsoid (Veras et al. 2014b) into `Mercury` for every system sampled to flag ejection, thereby allowing us to quantify escape in preferential directions. This ellipsoid is dependent on both the stellar mass and the Galactic tidal prescription used.

We use a slightly simplified version of the local field star mass function presented in Parravano et al. (2011) (see their Fig. 7), with a Solar neighbourhood-specific spatial stellar density of $n_\star = 0.392$ pc^{-3} and a stellar flyby distribution which is uniformly distributed in log mass such that $-1.2 \leqslant \ln(M_\mathrm{b}/M_\odot) \leqslant 0.1$. Here, M_b refers to the mass of the stellar flyby. We also simplify our model by adopting an encounter velocity of $V_\mathrm{b} = 45.7$ km/s, which corresponds with the expected mean velocity in the Solar neighbourhood (García-Sánchez et al. 2001).

Incoming stars are initially placed at a distance r_0 in a randomly chosen direction from the Sun. They perturb all the bodies of the simulation as point masses. Flyby stars are assumed to move in straight lines (i.e. with hyperbolic eccentricities of infinity) with speed V_b, also in a randomly-chosen direction (with $\vec{V}_\mathrm{b} \cdot \vec{r}_0 < 0$ so that the star initially travels towards the Sun)[3]. Stars spend an average time r_0/V_b within r_0 of the Sun. Consequently, during every integration timestep, of length Δt, we introduce a new star with probability

$$P_\mathrm{b} = \frac{4\pi}{3} n_\star r_0^2 V_\mathrm{b} \Delta t \quad (1)$$

so that the local stellar density is $n_\star$ on long timescales. The coefficient of $\frac{4}{3}$ is from our use of spherical geometry, rather than the cylindrical geometry of, e.g., Stern & Shull (1988). The value of Δt is determined by a Bulirsch-Stoer accuracy parameter of 10^{-13}. We chose $r_0 = 2.5 \times 10^5$ au, as encounters at larger distances are not expected to significantly affect the evolution.

4.2 Initial conditions

We perform 5 sets of 24 simulations of exo-Oort clouds lasting for 10 Gyr starting from the end of the main sequence. Each set contains a different stellar progenitor main sequence mass ($1M_\odot$, $2M_\odot$, $3M_\odot$, $4M_\odot$, $5M_\odot$). The stars are evolved in mass and radius according to the stellar evolution code `SSE` (Hurley et al. 2000), which assumes isotropic mass loss (see Section 2). The stars are assumed to have Solar metallicity. The duration of the mass loss phases for the stellar progenitors are, respectively, 1.431 Gyr, 331.6 Myr, 99.93 Myr, 36.11 Myr, and 17.51 Myr, and their eventual WD masses are $0.52M_\odot$, $0.64M_\odot$, $0.75M_\odot$, $0.87M_\odot$, and $1.00M_\odot$. For more details on the evolution of these particular stars see Veras et al. (2013a).

We model exo-Oort clouds with 5000 comets each, where each comet is treated as a test particle. These comets have semimajor axes which are distributed between 10^4 au and 10^5 au according to three power law distributions, a^{-1}, $a^{-3/2}$ and a^{-2}.

[3] Our approximation is robust because for curved trajectories, the pericentre velocity of the flyby stars closely mimics V_b unless the flyby star has an unusually slow and close orbit. For a stellar flyby eccentricity e_b, the pericentre velocity strays by more than 10% only in the special case of $1 < e_\mathrm{b} \lesssim 10.5$ and strays by over a factor of two only if $1 < e_\mathrm{b} < 5/3$.

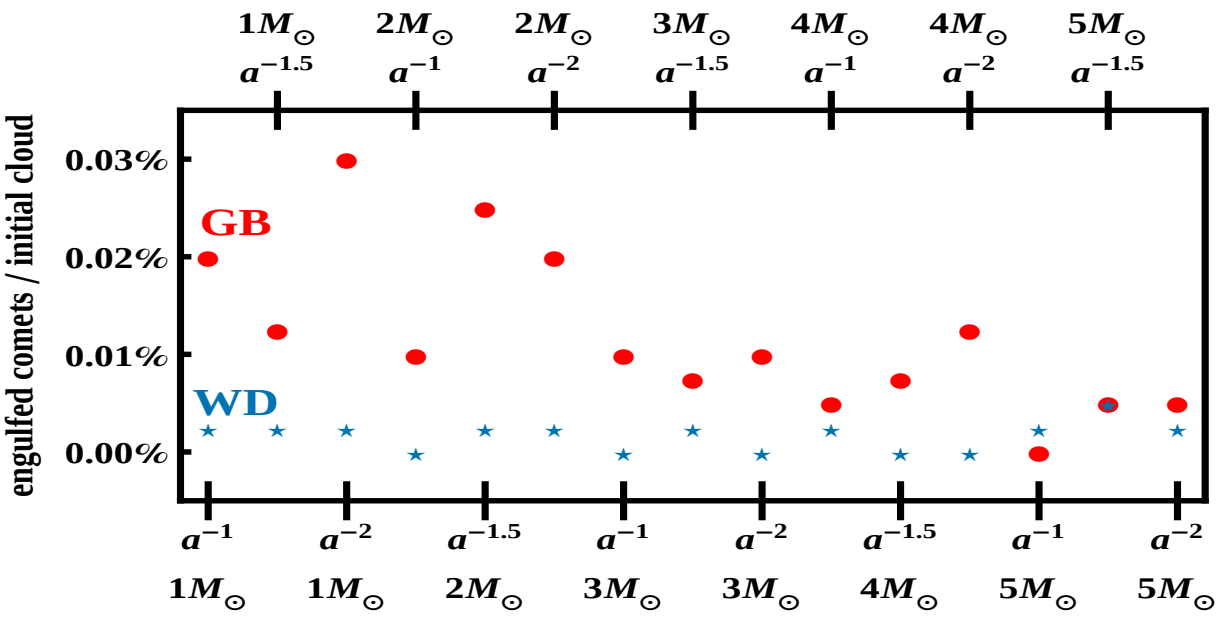

Figure 1. The fraction of comets in exo-Oort clouds which enter the Roche radius of the star when it is a giant branch star (GB; red filled dots) or a white dwarf (WD; blue stars). The results of all 120 simulations of 5000 comets each are presented, binned according to the main sequence stellar mass and semimajor axis profile of comets (shown on the top and bottom axes). About 87% of all engulfments by the star occur between the end of the main sequence and the beginning of the WD stage (the mass-losing phase). Hence, comets are expect to hit the WD at a rate of about one per 10^4 yr.

Each of the distributions accounts for 8 of the 24 simulations in each set. The comets' eccentricities, mean anomalies, longitudes of ascending node and arguments of pericentre are drawn from a uniform random distribution. The eccentricities of Oort cloud comets were originally assumed to be isotropically distributed (Oort 1950) because even if these comets once harboured high eccentricities, these eccentricities could have subseqently been damped through stellar flybys and Galactic tides. Because we assume the star is spherical, the comet's inclination is measured with respect to the Galactic plane. This value crucially dictates the strength of the Galactic tide. Therefore, we have sampled comets from a $\sin i$ distribution for $i = 0^\circ - 90^\circ$ and $i = 180^\circ - 270^\circ$, and from a $\sin(90^\circ - i)$ distribution for $i = 90^\circ - 180^\circ$ and $i = 270^\circ - 360^\circ$. Doing so helps prevent us from undersampling the phase space around the inclination values of 90° and 270°, which would cause the greatest orbital variation due to tides.

5 RESULTS

5.1 Exo-Oort cloud comets as a source of H-accretion

Our key result is illustrated in Fig. 1. This figure bins all of the simulations in 15 groups, for different radial comet profiles and progenitor main sequence stellar masses. For each bin, the figure displays the fraction of comets which have entered the Roche radius of the star throughout the simulations. The characteristic value is $\sim 0.01\%$. However, about 87% of these comet engulfments occur when the star is on the giant branch. Therefore, the characteristic engulfment fraction for WDs is $\sim 0.001\%$. These values may be higher by a factor of a couple for main sequence masses of $1 - 2M_\odot$.

Consequently, no more than 10^{-5} of an initial exo-Oort cloud should pollute the average WD. Therefore, for a typical main sequence exo-Oort cloud composed of 10^{11} comets, at most 10^6 comets could ever reach the WD over 10^{10} years. Hence, one comet intersects with the WD Roche radius every 10^4 years, which is the same order of magnitude predicted by Alcock et al. (1986). Figure 1 indicates that this result is relatively insensitive to stellar mass or the semimajor axis distribution of comets.

We can place these values in context by considering Fig. 7 of Raddi et al. (2014). Every WD on this plot which has accumulated more than 10^{22} g of H can be explained in our model as accretion from an exo-Oort cloud that is at least as massive as 10^{28} g. Many of the older WDs contain much more H, up to about 10^{25} g. These stars have accumulated their H from either rocky material like asteroids, particularly massive exo-Oort clouds, or a few particularly massive comets from an exo-Oort cloud (the mass distribution of the Solar system's long-period comets is top-heavy; Fernández & Sosa 2012).

Exo-Oort cloud masses are largely unconstrained observationally, although reasonable estimates can be obtained to within a couple orders of magnitude (as in e.g., Moro-Martín et al. 2009). We assume that these clouds have masses that are distributed about some median value which is

comparable to that in the Oort cloud. Further, the assumption that the Oort cloud is typical is congruent with observed planetary and protoplanetary systems and models of Oort cloud formation. Regardless, WDs are likely to accrete a large number of comets throughout their very long existence, and this process could significantly contribute to observed trace H in old He-atmosphere WDs. In addition, water-rich asteroids (e.g. Farihi et al. 2013; Raddi et al. 2014) provide an extra source of H; accretion from the interstellar medium, exo-Kuiper belts, and 'mini-exo-Oort clouds' (Raymond & Armitage 2013) may contribute to some extent as well. However, the fraction of water-ice which can survive post-main-sequence evolution may be a strong function of both size and distance (Stern et al. 1990; Jura & Xu 2010).

5.2 Exo-Oort cloud comets as a source of metal pollution

As some Oort cloud comets do contain metals in addition to H, we now consider the potential contribution of exo-Oort cloud comet accretion to the metal budget of WD atmospheres. We preface the computations with the caveat that the fraction of metals versus H in comets is largely unknown.

When a WD accretes metals, the metals will remain in the convective layer for as little as a few days, to as long as a few million years, depending on the composition of the envelope, and the temperature of the WD. As the depth of the convection zone can be calculated, a measurement of the abundances of metals in the atmosphere can be understood in terms of the total mass of metals in the convection zone, and thus, a lower bound for the total amount of metals accreted. Model inferences from observations find that the total mass of metals within deep convection zones of DBZ WDs is 10^{20-25} g (Girven et al. 2012) for those WDs with detectable amounts of pollution. Combined with the time for metals to sink out of the convective zone (see e.g. Paquette et al. 1986 and Koester 2009), a mass accretion rate of exo-Oort cloud comets can be derived.

Wyatt et al. (2014) performed this calculation. In doing so, they also observationally debiased the values from Girven et al. (2012), allowing them to fit a population model of small bodies accreted by WDs to the measurements of the total mass of metals within the deep convective layers. They were able to fit the observations with a log-normal distribution with a mean rate of $\dot{M} \approx 10^8$ g s^{-1}, and a standard deviation of $\sigma \approx 1.3$ dex. They also fit the size-number distribution of the small bodies as

$$n\,(>R) = n_0 R^{1-q} \quad (2)$$

for the number of small bodies n with radius greater than R, so that the population satisfies $q \approx 3$. This value is very close to the value found for long period comets ($q = 3.2 \pm 0.2$, Fernández & Sosa 2012), the asteroid belt and scattered disk ($q \approx 2.5$, Bottke et al. 2005; Vilenius et al. 2012), trans-Neptunian objects as a whole ($q \approx 4$, Trujillo et al. 2001; Fraser et al. 2008), and inferred for extrasolar small body populations ($q \sim 4$, Shannon & Wu 2011). Hence, a population of small bodies such as comets is compatible with the polluter population. If we assume that distributions of extrasolar comets and asteroids have the same q values as those in the Solar system, then $q \simeq 3$ does not allow us to differentiate between any of these populations of planetary bodies.

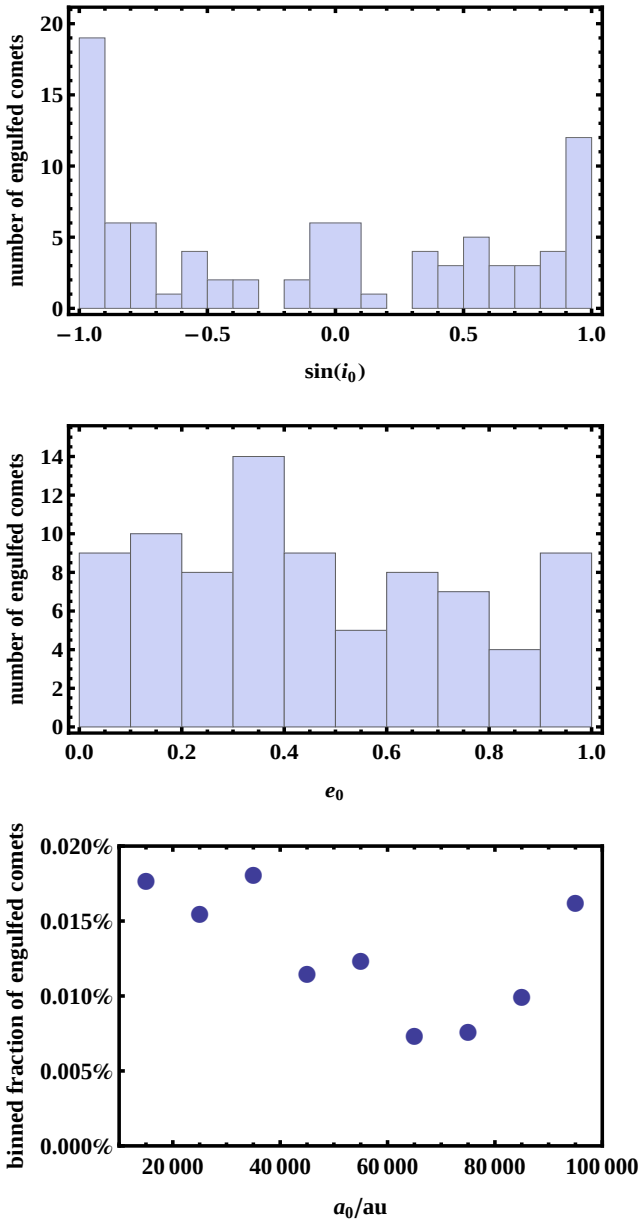

Figure 2. The initial distributions of the sines of the inclination, the eccentricities, and semimajor axes of all exo-Oort cloud comets which were engulfed across all simulations. The initial inclination distribution of the engulfed comets largely follows the initial inclination distribution of all comets, and the relatively flat eccentricity distribution exhibits a similar correlation. The nonzero values in each semimajor axis bin demonstrate that engulfment occurred across the range sampled.

However, producing the mass accretion rate found in Wyatt et al. (2014) by long-period comets is far more difficult. Our calculations found that roughly 10^{-5} of the primordial population was accreted by the WD over roughly 10^{10} yrs. Consequently, we obtain a mass accretion rate of 10^{-15} yr^{-1} = 3×10^{-23} s^{-1} of the primordial population. This rate would demand a mean Oort cloud mass of $\sim 3 \times 10^{30}$ g $\approx 500 M_\oplus$,

which is $10 - 100$ times the estimated mass of the Oort cloud (Weissman 1996; Dones et al. 2004; Francis 2005; Brasser 2008). Although the efficiency with which objects are implanted into the Oort cloud may be higher for systems with lower-mass planets (Lewis et al. 2013) and can depend on the stellar environment in which it is formed (Kaib & Quinn 2008; Brasser et al. 2012), even a formation channel with $\sim 100\%$ efficiency would still require a mass budget of ~ 10 times the Minimum Mass Solar Nebula (Weidenschilling 1977; Hayashi 1981). Five hundred earth masses of solids also exceeds by a factor of ~ 10 the total mass budget of solids available to a typical protoplanetary disk (Williams & Cieza 2011).

Although WD progenitors are somewhat more massive than the Sun on average, the mass of protoplanetary disks increases only linearly with the stellar mass (Williams & Cieza 2011). Thus while a $500 M_{\oplus}$ Oort cloud might be possible under the most optimistic of assumptions, it seems very difficult to produce such clouds as the mean of the population. When one considers the clouds which are one standard deviation above the mean value of ($\sim 10^4 M_{\oplus}$) even optimistic investigators would likely conclude that long-period comets cannot be the primary agents responsible for the observed metal pollution of WDs – which is consistent with the conclusions drawn from the abundance studies of the circumstellar debris (Sect. 2.1).

However, the accretion rate of 3×10^{-23} s^{-1} of the primordial population, when applied to estimated mass of the Oort cloud ($\sim 10 M_{\oplus}$) yields a mass accretion rate of $\sim 10^6$ g s^{-1}, just shy of the lowest detected rates in Wyatt et al. (2014). Thus, if the Solar System's Oort cloud is typical, we should expect to find WDs polluted by cometary material in the future from the high end tail of the exo-Oort cloud mass distribution tail.

5.2.1 Link to initial orbital properties

Now we take a closer look at the how the engulfment of exo-Oort cloud comets is correlated to their initial orbital properties in Figure 2. The figure shows that the distribution of the initial inclinations and eccentricities of the engulfed comets largely mirrors the initial distributions of all comets. Although comets with smaller semimajor axes are preferentially engulfed by the WD, the nonzero bins up to $a_0 = 10^5$ au demonstrate that the entire range of sampled initial semimajor axes yield engulfed comets.

Some combination of Galactic tides and flybys could play a significant role in particular systems. The systems in the two bins closest to $\sin i_0 = \pm 1$ would be most affected by vertical tides. The nonzero bins surrounding $\sin i_0 = 0$ raise the possibility that the radial Galactic tides by themselves are strong enough to produce engulfment, or that flybys are the dominant driver of engulfment in those cases. Kaib & Raymond (2014) note that achieving a pericentre which causes star-star collisions from wide binaries is primarily due to external stellar flybys, because tidally changing the pericentre becomes more difficult as the pericentre approaches zero. Their pericentre value of about a Solar radius is similar to the Roche radius of a typical WD that we adopt here, and so their result should hold here also. However, their statement is true only for vertical tides, as the dependence of eccentricity on radial tides is complex (e.g. equation A2 of Veras & Evans 2013). In fact, Fig. 8 of Levison et al. (2006) shows how radial tides can drive the pericentre down by a factor of 2.

5.2.2 Dissipation of the exo-Oort cloud

During and after the giant branch phases, the exo-Oort cloud is decimated. Although our WD Roche radius collision rate is similar to the overall collision rate of Alcock et al. (1986), we differ on our estimates for the retention of Oort cloud comets during mass loss. Our results for exo-Oort cloud retention are significantly more pessimistic. Alcock et al. (1986) suggest that over half of the long-period, highly eccentric comets are retained during mass loss. We find that over half of our exo-Oort clouds are retained during mass loss for only a subset of our simulations with a progenitor main sequence stellar mass of $1 M_{\odot}$. Even for those simulations, less than 15% of the Oort cloud is retained after 2 Gyr of WD cooling.

The primary reasons for the disagreement are model-dependent. Some factors are our use of a Hill escape ellipsoid rather than an escape sphere, the different orbital distribution of comets at the start of mass loss, the presence of flybys during mass loss, and potentially the different stellar evolution profiles we use for a variety of stellar masses (although Alcock et al. 1986 do consider a wide range of total mass lost and adiabaticity). The key factor perhaps is that highly nonadiabatic mass loss at the tip of the asymptotic giant branch typically raises the semimajor axis of a comet by a factor which is higher than a few (Veras et al. 2011), and consequently ejects the comet either during mass loss or soon after (within one orbit). The combination of orbital expansion and Hill ellipsoid shrinkage when a star becomes a WD means that 51%-88% of the volume of the entire main sequence Hill ellipsoid is a danger zone that will later eject any occupants (see Section 5.1 and Fig. 6 of Veras et al. 2014b).

We illustrate the time-dependent ejection of the exo-Oort clouds for the lowest stellar mass case in Fig. 3. In all other cases, over 80% of the cloud is ejected when the star begins life as a WD. The figure displays three sets of 8 cumulative overlaid histograms of the ejection fraction of the original exo-Oort cloud with respect to the time when the star becomes a WD. The survival time of the cloud correlates with the steepness of the initial semimajor axis profile. When comets are initially concentrated away from the edge of the Hill ellipsoid, they are likely to survive for longer. The oldest metal polluted WDs, with cooling ages of about 5 Gyr (Farihi et al. 2011; Koester et al. 2011), can expect to have retained no more than 5% of the cloud which existed at the beginning of the giant branches.

Each plot shows significant variation amongst some of the overlaid histograms. The most dramatic differences occur for the topmost curves on the $a^{-1.5}$ and a^{-2} plots, where nearly the entire cloud escapes about 1 Gyr before the star becomes a WD, and when the star still contains over 99.95% of its original mass. The sudden escape in these systems is caused by a highly intrusive flyby at, respectively, 225 Myr and 379 Myr after the start of the simulation. The flybys penetrate to pericentre distances of 394 au and 528 au. Figure 4 is a correctly-scaled Cartesian plot of the points of escape for all comets in the corresponding $a^{-1.5}$ simulation. The dense blue patch in the upper-right portion of the ellipsoid is the actual location where most comets escape during the intrusion. This patch results in a highly inhomogeneous escape distribution.

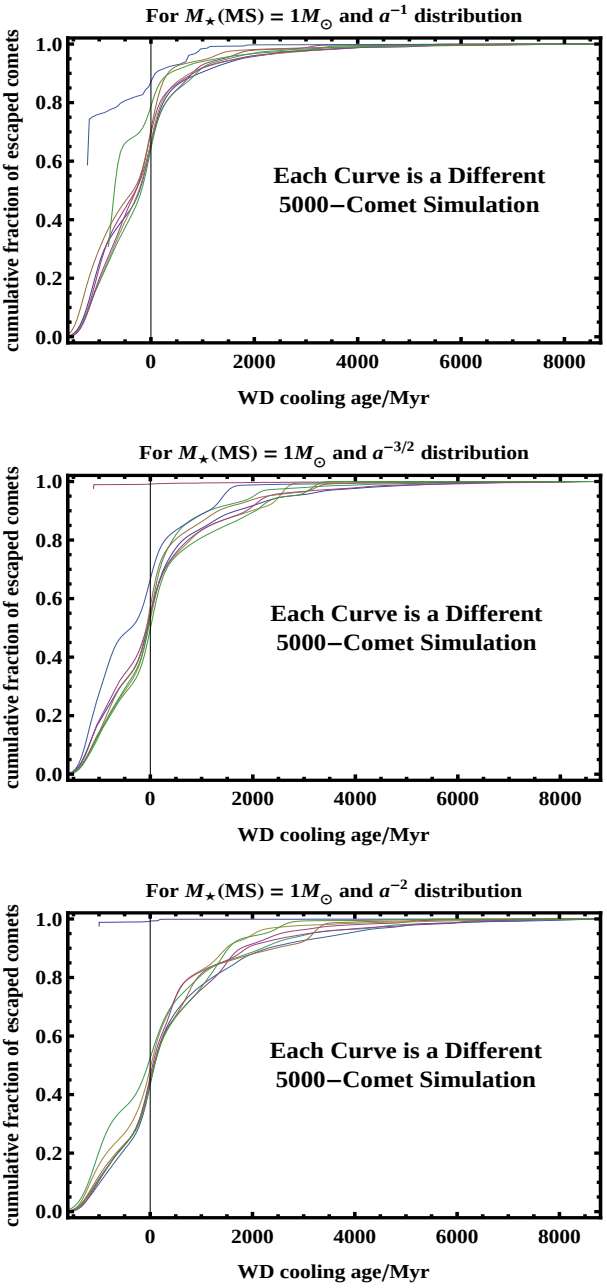
For $M_\star$(MS) = $1M_\odot$ and a^{-1} distribution
cumulative fraction of escaped comets
Each Curve is a Different 5000−Comet Simulation
WD cooling age/Myr
For $M_\star$(MS) = $1M_\odot$ and $a^{-3/2}$ distribution
cumulative fraction of escaped comets
Each Curve is a Different 5000−Comet Simulation
WD cooling age/Myr
For $M_\star$(MS) = $1M_\odot$ and a^{-2} distribution
cumulative fraction of escaped comets
Each Curve is a Different 5000−Comet Simulation
WD cooling age/Myr

Figure 3. Cloud dissipation: the cumulative distributions of escaped exo-Oort cloud comets as a function of time for all simulations with a $1M_\odot$ main sequence progenitor stellar mass. Each plot corresponds to a different initial semimajor axis distribution of comets and contains 8 curves. All curves illustrate that the exo-Oort cloud is at least 95% depleted by WD cooling ages of 5 Gyr. For earlier cooling ages, typically less than half of the comets remain in the cloud. For higher progenitor stellar masses, the cloud depletes at a faster rate.

We should actually expect such intrusions to occur with pericentres of a few hundred au in a fraction of all systems. Both Zakamska & Tremaine (2004) and Veras & Moeckel (2012) demonstrate that one such close star-star pericentre passage should occur on average once during a ~ 10 Gyr main sequence lifetime. Hence, we should expect a similarly disruptive event during 10 Gyr of WD evolution.

Although the lowest mass case is illustrative of the relevant dynamics, the majority of currently observed WDs did not evolve from Solar-mass main-sequence stars (see Fig. 1 of Koester et al. 2014). Hence, determining how the reservoir of available exo-Oort cloud comets is depleted as a function of stellar mass is important. Figure 5 showcases this dependence for the representative a^{-2} initial power-law distribution of exo-Oort cloud comets. The dependence is steep, particularly as the progenitor stellar mass is increased from $1M_\odot$ to $3M_\odot$. Consequently, we expect the accumulation of H due to exo-Oort cloud comets to be a function of both the WD mass itself, and its cooling age.

6 DISCUSSION

6.1 Observing cometary accretion

In contrast to accretion of rocky material, an ongoing process which is currently observed, we have not yet detected the accretion of cometary, volatile material onto WDs. Two reasons are (1) entry into the WD Roche radius is potentially less frequent for exo-Oort cloud comets than for asteroids, and (2) the different lifetimes of the gaseous disc – produced from the sublimation of a frozen iceball (comet) – and the dusty disc, produced from the tidal disruption of a dry rocky asteroid. The key parameter for the subsequent of the evolution of these discs is their viscosity, which is much higher for the gaseous discs compared than for dusty discs. Dusty discs have an estimated lifetime of $\sim 10^{4.5} - 10^{6.5}$ yr (Girven et al. 2012) whereas gaseous discs sustain themselves for only a few 10^3 yr (Metzger et al. 2012) (see also Jura 2008 for estimates of the gas/dust disc life times). Bearing in mind that about 30 WDs with dust disc detections are currently known, it is unsurprising that we have not yet identified an unambiguous case of ongoing accretion from a tidally disrupted comet.

6.2 Progenitors of metal pollutants

Regarding sourcing metal pollution in WD atmospheres, the outcome of this study emphasises the need to pursue other avenues of investigation. Considerations of the debris abundances aside, the dynamics of injecting comets from exo-Oort clouds orbiting WDs into the Roche radii of the WDs cannot explain the mass accumulated over convective timescales in DBZ WDs. The contribution of these comets to the pollution is negligible unless we are underestimating the typical masses of exo-Oort clouds by several orders of magnitude.

Other potential metal pollutant progenitors are planets, moons or asteroids. Planets are unlikely because the frequency of direct collisions with the WD is too low (Debes & Sigurdsson 2002; Veras et al. 2013a; Voyatzis et al. 2013; Mustill et al. 2014). Asteroids and Kuiper-belt-like objects have also been the subject of recent investigation. Bonsor et al. (2011) demonstrate that scattering between a planet and an exo-Kuiper belt during the giant branch phases of evolution can generate a sufficient quantity of mass in the inner planetary system to match heavy metal accretion rates, but do not model how this mass obtains

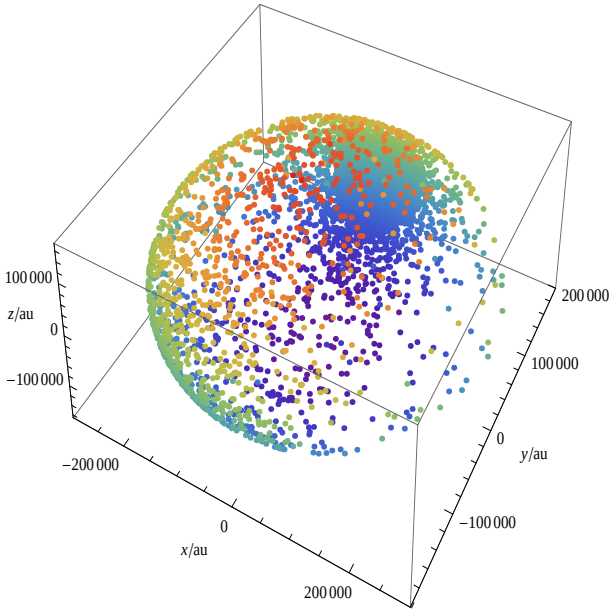

Figure 4. Patchy escape due to an intrusive stellar flyby: the Cartesian (x, y, z) locations where comets escape the Hill ellipsoid for a single 5000-comet 10 Gyr simulation with a stellar progenitor mass of $1M_{\odot}$ and an initial exo-Oort cloud distribution of semimajor axes of $a^{-3/2}$. The simulation corresponds to the topmost (crimson) curve in the middle panel of Figure 3. The colours of the dots correspond to different values of z, with the highest values in red and the lowest in violet. The blue patch of escaping comets at high y and low (x, z) occurs about 225 Myr along the giant branch phase, well before any significant mass loss occurs. This patch is due to a flyby star penetrating to a closest-approach distance of just 394 au at that time.

WD-grazing orbits. Debes et al. (2012) and Frewen & Hansen (2014) show how resonant diffusion between a planet and an exo-asteroid belt can represent an effective mechanism to transfer asteroids to the WD Roche radius, but do not perform simulations past 1 Gyr, and suggest that super-exo-asteroid belt masses are required to explain the observations. Further, a debris field generated by the rotational break-up of asteroids from giant star radiation (Veras et al. 2014c) could affect the size distributions of potentially polluting bodies. Sub-metre-sized particles could be dragged inward during giant branch envelope evolution and be available as pollutants (Dong et al. 2010), but probably would not exist in sufficient quantities to account for the observed accreted mass. Overall, none of theoretical models has yet to provide a complete explanation of the observations.

6.3 Simulation subtleties

Our results here are model-dependent, which is why we have taken a Monte-Carlo approach to our simulations. The structure of an exo-Oort cloud at the start of the giant branch phases is unknown, as is the structure at the start of the main sequence. Although all of our comets initially harboured semimajor axes greater than 10^4 au, mechanisms which produce Sedna and other inner Oort cloud objects rely on planets (e.g. Gomes et al. 2006; Gladman & Chan 2006; Lewis et al. 2013), or the Sun's birth environment (Brasser et al. 2006; Levison et al. 2010), or migration within the galaxy (Kaib et al. 2011). These mechanisms can

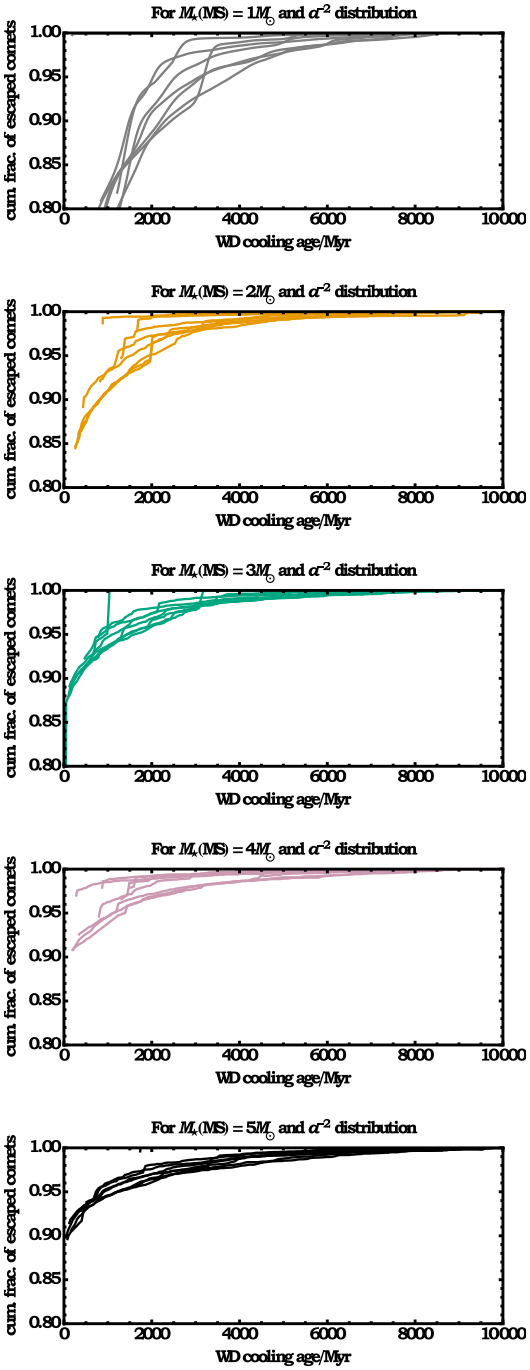

Figure 5. Like Fig. 3, except as a function of stellar mass. Note that all y-axes here range from 80%-100%. The figure demonstrates a steep dependence on stellar mass; for progenitor masses greater than $3M_{\odot}$, all exo-Oort clouds are already at least 90% depleted by the time the star becomes a WD.

allow for speculation on whether the Sun's cloud is typical, but exploring them comprehensively is computationally prohibitive.

Our result is resolution-limited, as on average we see one WD Roche radius engulfment for every two simulations. However, including 5000 comets per simulation already pushes current computational resources. We succeeded in integrating so

many comets amidst mass loss for 10 Gyr because their wide orbits allow the integrator to use timesteps which are orders of magnitude larger than those from planetary simulations. Inserting planets in our simulations is not feasible because of the prohibitive timestep constraints they would introduce. Further, they would force us to reduce the number of comets per simulation to the extent that we might not see any engulfment at all.

6.4 The effect of planets

As just mentioned, planetary influences may be a key factor in explaining accretion rates in systems with asteroid or Kuiper belts. Their influence on exo-Oort clouds, however, is not as impactful.

We did not include planetary systems, as the computation demands of integrating short period orbits (and a larger number of massive bodies) is prohibitive. However, Oort clouds are initially created by the gravitational scattering of planets (Oort 1950). Such a planetary system might influence the evolution of the comet orbits near the star, altering the rate at which comets enter the Roche radius. Horner et al. (2010), for instance, found that the flux of Oort cloud comets into the terrestrial planet region of the solar system is reduced by a factor of a few by Jupiter, compared to a system with a less massive planet in its place, as Jupiter can effectively eject incoming Oort cloud comets. A similar result is found by Lewis et al. (2013), who find that systems with a Saturn-mass planet or higher can reduce the rate Oort cloud comets get into the inner solar system by a factor of a few. Saturn mass planets (and larger) occur around $\sim 10\%$ of Sun-like stars (Mayor et al. 2011) in periods of less than ~ 10 years, while longer periods have not been effectively probed by any detection method, and $\sim 10\%$ of A-stars have planets of a few Jupiter masses at separations of 5-300 au (Vigan et al. 2012). This potential depletion is mitigated by uncertainties about the survival of planetary systems. Planetary systems may be unstable during the main-sequence lifetime of stars (Chambers et al. 1996; Jurić & Tremaine 2008), a problem that can be compounded by the post-main-sequence evolution (Veras et al. 2013a; Mustill et al. 2014), and can of course be lost to the star directly during post-main-sequence evolution (Mustill & Villaver 2012). The necessity that a planetary system be there to form an Oort cloud does not mean it must persist through the WD phase. The overall uncertainty in our predictions from not including planetary systems is thus perhaps a factor of a few; in the worst case it may approach an order of magnitude.

6.5 Other dynamical considerations

Other effects not included in our simulations are stellar-comet tides nor general relativity. For a single periastron passage, stellar tides would not affect whether the comet enters the Roche radius. Further, these tides will not have time to act over multiple orbits because the orbit is likely to change, particularly at apastron, due to Galactic tides and stellar flybys. General relativity will push the comet away from the star at closest approach on the order of 4 km $\times(M_\star/M_\odot)$ (Veras 2014), and so has a negligible effect in our simulations here.

The dynamical mechanisms discussed in this work are also applicable to exo-Oort clouds around stars which undergo supernovae. The only differences are that the rate of mass loss is much higher (see discussion in Section 3.3.4 of Veras et al. 2011), the total amount of mass loss may be higher, and that the parent star will become either a neutron star or black hole. Hills (1983) provides an extensive analysis of how the orbital elements of secondaries which orbit exploding stars change due to instantaneous mass loss. In his Section III-d-iii, he describes the specific outcomes of comets, and estimates that only after several Gyr would passing stars drive down the pericentre of some surviving comets enough to hit the neutron star.

If in the future we are able to probe WDs outside of the Solar neighbourhood, then the comet pollution hypothesis may be worth revisiting. Most WDs in the Milky Way are between the Solar neighbourhood and the Galactic bulge. Galactic tides towards the bulge cause eccentricity oscillations with a greater frequency than those in the Solar neighbourhood and are not dominated by vertical tides (Veras & Evans 2013). Further, towards the bulge, the stellar flybys are more frequent *and* the three Hill ellipsoid axes are all smaller than in the Solar neighbourhood for a given stellar mass.

7 SUMMARY

Atmospheric hydrogen represents a permanent historical tracer of WD accretion activity. We have performed a dynamical analysis of post-main-sequence exo-Oort clouds to determine their contribution to the accreted circumstellar mass observed in WD atmospheres. We find that comets infrequently but gradually increase the H budget in WD atmospheres. Galactic tides, stellar flybys, and the location of the Solar neighbourhood in the Milky Way all conspire to yield an exo-Oort cloud engulfment fraction of 10^{-5}. One can use this value in conjunction with an assumed exo-Oort cloud mass and WD atmosphere heavy metal mass total (which can reach 10^{25} g) to speculate about the accretion history of these stars on a case-by-case basis.

ACKNOWLEDGEMENTS

We thank the referee for a thorough and helpful review of the manuscript. We also thank Alan P. Jackson, Jay Farihi and Roberto Raddi for useful discussions. The research leading to these results has received funding from the European Research Council under the European Union's Seventh Framework Programme (FP/2007-2013) / ERC Grant Agreement n. 320964 (WDTracer) and n. 279973 (DEBRIS). DV and BTG are funded under WDTracer, and AS is funded under DEBRIS.

REFERENCES

Aannestad, P. A., Kenyon, S. J., Hammond, G. L., & Sion, E. M. 1993, AJ, 105, 1033
Alcock, C., Fristrom, C. C., & Siegelman, R. 1986, ApJ, 302, 462
Alcock, C., & Illarionov, A. 1980, ApJ, 235, 541
Allègre, C., Manhès, G., & Lewin, É. 2001, Earth and Planetary Science Letters, 185, 49

Althaus, L. G., Serenelli, A. M., Panei, J. A., et al. 2005, A&A, 435, 631
Asplund, M., Grevesse, N., Sauval, A. J., & Scott, P. 2009, ARA&A, 47, 481
Bear, E., & Soker, N. 2013, New Astronomy, 19, 56
Becklin, E. E., Farihi, J., Jura, M., et al. 2005, ApJL, 632, L119
Bergeron, P., Wesemael, F., Dufour, P., et al. 2011, ApJ, 737, 28
Bergfors, C., Farihi, J., Dufour, P., & Rocchetto, M. 2014, MNRAS, 444, 2147
Bonsor, A., Mustill, A. J., & Wyatt, M. C. 2011, MNRAS, 414, 930
Bottke, W. F., Durda, D. D., Nesvorný, D., et al. 2005, Icarus, 175, 111
Brasser, R. 2001, MNRAS, 324, 1109
Brasser, R., Duncan, M. J., & Levison, H. F. 2006, Icarus, 184, 59
Brasser, R. 2008, A&A, 492, 251
Brasser, R., Duncan, M. J., Levison, H. F., Schwamb, M. E., & Brown, M. E. 2012, Icarus, 217, 1
Brinkworth, C. S., Gänsicke, B. T., Marsh, T. R., Hoard, D. W., & Tappert, C. 2009, ApJ, 696, 1402
Brinkworth, C. S., Gänsicke, B. T., Girven, J. M., et al. 2012, ApJ, 750, 86
Brown, J. C., Potts, H. E., Porter, L. J., & Le Chat, G. 2011, A&A, 535, A71
Chambers, J. E. 1999, MNRAS, 304, 793
Chambers, J. E., Wetherill, G. W., & Boss, A. P. 1996, Icarus, 119, 261
Debes, J. H., & Sigurdsson, S. 2002, ApJ, 572, 556
Debes, J. H., Walsh, K. J., & Stark, C. 2012, ApJ, 747, 148
Dones, L., Weissman, P. R., Levison, H. F., & Duncan, M. J. 2004, Star Formation in the Interstellar Medium: In Honor of David Hollenbach, 323, 371
Dong, R., Wang, Y., Lin, D. N. C., & Liu, X.-W. 2010, ApJ, 715, 1036
Dufour, P., Bergeron, P., Liebert, J., et al. 2007, ApJ, 663, 1291
Farihi, J., Jura, M., & Zuckerman, B. 2009, ApJ, 694, 805
Farihi, J., Barstow, M. A., Redfield, S., Dufour, P., & Hambly, N. C. 2010, MNRAS, 404, 2123
Farihi, J., Dufour, P., Napiwotzki, R., & Koester, D. 2011, MNRAS, 413, 2559
Farihi, J., Gänsicke, B. T., Steele, P. R., et al. 2012, MNRAS, 421, 1635
Farihi, J., Gänsicke, B. T., & Koester, D. 2013, Science, 342, 218
Fernández, J. A., & Sosa, A. 2012, MNRAS, 423, 1674
Fontaine, G., & Michaud, G. 1979, ApJ, 231, 826
Francis, P. J. 2005, ApJ, 635, 1348
Fraser, W. C., Kavelaars, J. J., Holman, M. J., et al. 2008, Icarus, 195, 827
Frewen, S. F. N., & Hansen, B. M. S. 2014, MNRAS, 439, 2442
Friedrich, S., Jordan, S., & Koester, D. 2004, A&A, 424, 665
Gänsicke, B. T., Marsh, T. R., Southworth, J., & Rebassa-Mansergas, A. 2006, Science, 314, 1908
Gänsicke, B. T., Marsh, T. R., & Southworth, J. 2007, MNRAS, 380, L35
Gänsicke, B. T., Koester, D., Marsh, T. R., Rebassa-Mansergas, A., & Southworth, J. 2008, MNRAS, 391, L103
Gänsicke, B. T. 2011, American Institute of Physics Conference Series, 1331, 211
Gänsicke, B. T., Koester, D., Farihi, J., et al. 2012, MNRAS, 424, 333
García-Sánchez, J., Weissman, P. R., Preston, R. A., et al. 2001, A&A, 379, 634
Girven, J., Brinkworth, C. S., Farihi, J., et al. 2012, ApJ, 749, 154
Gladman, B., & Chan, C. 2006, ApJL, 643, L135
Gladman, B. J., Migliorini, F., Morbidelli, A., et al. 1997, Science, 277, 197
Gomes, R. S., Matese, J. J., & Lissauer, J. J. 2006, Icarus, 184, 589
Graham, J. R., Matthews, K., Neugebauer, G., & Soifer, B. T. 1990, ApJ, 357, 216
Hadjidemetriou, J. D. 1963, Icarus, 2, 440
Hayashi, C. 1981, Progress of Theoretical Physics Supplement, 70, 35
Heisler, J., & Tremaine, S. 1986, Icarus, 65, 13
Hills, J. G. 1983, ApJ, 267, 322
Horner, J., Jones, B. W., & Chambers, J. 2010, International Journal of Astrobiology, 9, 1
Hurley, J. R., Pols, O. R., & Tout, C. A. 2000, MNRAS, 315, 543
Jessberger, E. K., Christoforidis, A., & Kissel, J. 1988, Nature, 332, 691
Jiménez-Torres, J. J., Pichardo, B., Lake, G., & Throop, H. 2011, MNRAS, 418, 1272
Jura, M. 2003, ApJL, 584, L91
Jura, M. 2006, ApJ, 653, 613
Jura, M. 2008, AJ, 135, 1785
Jura, M., Muno, M. P., Farihi, J., & Zuckerman, B. 2009, ApJ, 699, 1473
Jura, M., & Xu, S. 2010, AJ, 140, 1129
Jura, M. 2011, AJ, 141, 155
Jura, M., & Xu, S. 2012, AJ, 143, 6
Jura, M., Xu, S., Klein, B., Koester, D., & Zuckerman, B. 2012, ApJ, 750, 69
Jurić, M., & Tremaine, S. 2008, ApJ, 686, 603
Kaib, N. A., & Quinn, T. 2008, Icarus, 197, 221
Kaib, N. A., Roškar, R., & Quinn, T. 2011, Icarus, 215, 491
Kaib, N. A., & Raymond, S. N. 2014, ApJ, 782, 60
Kilic, M., von Hippel, T., Leggett, S. K., & Winget, D. E. 2005, ApJL, 632, L115
Kilic, M., & Redfield, S. 2007, ApJ, 660, 641
Kimeswenger, S., Zijlstra, A. A., van Hoof, P. A. M., et al. 2008, arXiv:0804.4058
Klein, B., Jura, M., Koester, D., Zuckerman, B., & Melis, C. 2010, ApJ, 709, 950
Klein, B., Jura, M., Koester, D., & Zuckerman, B. 2011, ApJ, 741, 64
Koester, D. 1976, A&A, 52, 415
Koester, D. 2009, A&A, 498, 517
Koester, D., Girven, J., Gänsicke, B. T., & Dufour, P. 2011, A&A, 530, A114
Koester, D. 2013, Planets, Stars and Stellar Systems. Volume 4: Stellar Structure and Evolution, 559
Koester, D., Gänsicke, B. T., & Farihi, J. 2014, A&A, 566, A34
Knight, M. M., A'Hearn, M. F., Biesecker, D. A., et al. 2010, AJ, 139, 926
Lamy, P., Faury, G., Llebaria, A., et al. 2013, Icarus, 226, 1350

Lewis, A. R., Quinn, T., & Kaib, N. A. 2013, AJ, 146, 16
Levison, H. F., Duncan, M. J., Dones, L., & Gladman, B. J. 2006, Icarus, 184, 619
Levison, H. F., Duncan, M. J., Brasser, R., & Kaufmann, D. E. 2010, Science, 329, 187
Lodders, K. 2003, ApJ, 591, 1220
Mayor, M., Marmier, M., Lovis, C., et al. 2011, arXiv:1109.2497
Melis, C., Jura, M., Albert, L., Klein, B., & Zuckerman, B. 2010, ApJ, 722, 1078
Melis, C., Dufour, P., Farihi, J., et al. 2012, ApJL, 751, L4
Metzger, B. D., Rafikov, R. R., & Bochkarev, K. V. 2012, MNRAS, 423, 505
Minton, D. A., & Malhotra, R. 2010, Icarus, 207, 744
Moro-Martín, A., Turner, E. L., & Loeb, A. 2009, ApJ, 704, 733
Mustill, A. J., & Villaver, E. 2012, ApJ, 761, 121
Mustill, A. J., Veras, D., & Villaver, E. 2014, MNRAS, 437, 1404
Omarov, T. B. 1962, Izv. Astrofiz. Inst. Acad. Nauk. KazSSR, 14, 66
Oort, J. H. 1950, BAIN, 11, 91
Paquette, C., Pelletier, C., Fontaine, G., & Michaud, G. 1986, ApJS, 61, 197
Parravano, A., McKee, C. F., & Hollenbach, D. J. 2011, ApJ, 726, 27
Parriott, J., & Alcock, C. 1998, ApJ, 501, 357
Raddi, R. et al., 2014 In Prep
Rafikov, R. R. 2011a, MNRAS, 416, L55
Rafikov, R. R. 2011b, ApJL, 732, L3
Rafikov, R. R., & Garmilla, J. A. 2012, ApJ, 760, 123
Raymond, S. N., & Armitage, P. J. 2013, MNRAS, 429, L99
Reach, W. T., Kuchner, M. J., von Hippel, T., et al. 2005, ApJL, 635, L161
Schatzman, E. L. 1958, Amsterdam, North-Holland Pub. Co.; New York, Interscience Publishers.
Sekanina, Z., & Kracht, R. 2013, ApJ, 778, 24
Shannon, A., & Wu, Y. 2011, ApJ, 739, 36
Shannon, A., Clarke, C., & Wyatt, M. 2014a, MNRAS, 442, 142
Shannon, A., Jackson A. P., Veras, D., & Wyatt, M. 2014b, MNRAS, Submitted (MN-14-2536)
Sion, E. M., Greenstein, J. L., Landstreet, J. D., et al. 1983, ApJ, 269, 253
Stern, S. A., & Shull, J. M. 1988, Nature, 332, 407
Stern, S. A., Shull, J. M., & Brandt, J. C. 1990, Nature, 345, 305
Stone, N., Metzger, B., & Loeb, A. 2014, arXiv:1404.3213
Trujillo, C. A., Jewitt, D. C., & Luu, J. X. 2001, AJ, 122, 457
Vauclair, G., Vauclair, S., & Greenstein, J. L. 1979, A&A, 80, 79
Veras, D., Wyatt, M. C., Mustill, A. J., Bonsor, A., & Eldridge, J. J. 2011, MNRAS, 417, 2104
Veras, D., & Moeckel, N. 2012, MNRAS, 425, 680
Veras, D., & Wyatt, M. C. 2012, MNRAS, 421, 2969
Veras, D., & Evans, N. W. 2013, MNRAS, 430, 403
Veras, D., Mustill, A. J., Bonsor, A., & Wyatt, M. C. 2013a, MNRAS, 431, 1686
Veras, D., Hadjidemetriou, J. D., & Tout, C. A. 2013b, MNRAS, 435, 2416
Veras, D., Leinhardt, Z. M., Bonsor, A., & Gänsicke, B. T. 2014a, MNRAS, In Press, arXiv:1409.2493
Veras, D., Evans, N. W., Wyatt, M. C., & Tout, C. A. 2014b, MNRAS, 437, 1127
Veras, D., Jacobson, S. A., & Gänsicke, B. T. 2014c, MNRAS, In Press, arXiv:1409.4412
Veras, D. 2014, MNRAS, 442, L71
Vigan, A., Patience, J., Marois, C., et al. 2012, A&A, 544, A9
Vilenius, E., Kiss, C., Mommert, M., et al. 2012, A&A, 541, A94
Voss, B., Koester, D., Napiwotzki, R., Christlieb, N., & Reimers, D. 2007, A&A, 470, 1079
Voyatzis, G., Hadjidemetriou, J. D., Veras, D., & Varvoglis, H. 2013, MNRAS, 430, 3383
Weidenschilling, S. J. 1977, Ap&SS, 51, 153
Weissman, P. R. 1996, Completing the Inventory of the Solar System, 107, 265
Wesemael, F. 1979, A&A, 72, 104
Williams, J. P., & Cieza, L. A. 2011, ARA&A, 49, 67
Wilson, D. J, Gaensicke, B., Koester, D., et al. 2014, MNRAS, In Press, arXiv:1409.2490
Wyatt, M. C., Farihi, J., Pringle, J. E., & Bonsor, A. 2014, MNRAS, 439, 3371
Xu, S., Jura, M., Klein, B., Koester, D., & Zuckerman, B. 2013, ApJ, 766, 132
Xu, S., Jura, M., Koester, D., Klein, B., & Zuckerman, B. 2014, ApJ, 783, 79
Zakamska, N. L., & Tremaine, S. 2004, AJ, 128, 869
Zuckerman, B., & Becklin, E. E. 1987, Nature, 330, 138
Zuckerman, B., Koester, D., Reid, I. N., Hünsch, M. 2003, ApJ, 596, 477
Zuckerman, B., Koester, D., Melis, C., Hansen, B. M., & Jura, M. 2007, ApJ, 671, 872
Zuckerman, B., Melis, C., Klein, B., Koester, D., & Jura, M. 2010, ApJ, 722, 725